



A series of nonsecosteroidal vitamin D receptor agonists for osteoporosis therapy

Hirota Kashiwagi*, Yoshiyuki Ono, Masateru Ohta, Susumu Itoh, Fumihiko Ichikawa, Suguru Harada, Satoshi Takeda, Nobuo Sekiguchi, Masaki Ishigai, Tadakatsu Takahashi

Research Division, Chugai Pharmaceutical Co., Ltd, 1-135 Komakado, Gotemba, Shizuoka 412-8513, Japan

ARTICLE INFO

Article history:

Received 26 November 2012

Revised 16 January 2013

Accepted 18 January 2013

Available online 8 February 2013

Keywords:

Vitamin D₃

VDR agonist

Nonsecosteroid

Osteoporosis

CH5036249

ABSTRACT

In an extension of our study on gamma hydroxy carboxylic acid analogs, we explored a series of nonsecosteroidal vitamin D receptor (VDR) agonists in which 1,3-diol of 1,25(OH)₂D₃ had been replaced by aryl acetic acid. These analogs showed very potent activity in vitro compared with 1,25(OH)₂D₃. An X-ray analysis of **8d** showed that the inserted phenyl ring well mimicked the folded methylene linker of the gamma hydroxy carboxylic acid moiety but the carboxylic acid of **8d** interacted with VDR in a different manner from gamma hydroxy carboxylic acids. Through our in vivo screening in an osteoporosis rat model using immature rats, we identified a potent active vitamin D₃ analog, compound **7e**. In mature rats of the same model, compound **7e** also showed good PK profiling and excellent ability to prevent bone mineral density loss without severe hypercalcemia. Our nonsecosteroidal VDR agonist **7e** (CH5036249) could be a possible new drug candidate for treating osteoporosis in human.

© 2013 Elsevier Ltd. All rights reserved.

1. Introduction

Osteoporosis is a disease related to a decrease of bone mineral density (BMD), and the increased bone fragility in patients with this disease often causes bone fractures.¹ Especially in the case of elderly postmenopausal women, bone fracture is linked to patients becoming bedridden with long-term care requirement and suffering a remarkably decreased quality of life (QOL). Prevention and treatment are important for improving the QOL of the aging population worldwide.

In bone, calcium is the most important component, and calcium deficiency, which is a major risk factor for osteoporosis is caused by a decrease in vitamin D. Adequate intake of vitamin D and calcium is recommended as a baseline therapy for prevention and as a treatment for all osteoporosis patients. Evidence suggests that vitamin D supplementation may have favorable effects on BMD and even reduce the risk of fracture.^{2–10} Furthermore, alfacalcidol (1 α -hydroxyvitamin D₃, **1**), a prodrug of active vitamin D₃ (calcitriol, 1 α ,25-dihydroxyvitamin D₃ [1 α ,25(OH)₂D₃], **2**) is an efficacious and safe medication for the prevention and treatment of osteoporosis that has been used in clinics in Japan for more than 25 years. To improve upon this existing therapy, we pursued studies in secosteroidal vitamin D₃ analogs and identified the analog eldelcalcitol (**3**).¹¹ Edelcalcitol, which was approved in Japan as a new osteoporosis treatment drug last year, shows greater increase

in bone mass than alfacalcidol and comparable calcium absorption and parathyroid hormone levels in osteoporosis model rats.^{12,13} In a 12-month phase II study (218 patients), eldelcalcitol dose-dependently increased BMD in lumbar spine and hip and in a 3-year phase III study (1054 patients), eldelcalcitol, which has a safety profile similar to alfacalcidol, was more efficacious in preventing vertebral fracture in osteoporotic patients.^{14–17}

Because the calcemic effect of VDR agonists generally limits the dose it is possible to give in clinic, we were prompted to search for novel chemical class of VDR agonist for osteoporosis therapy, and discovering a potent VDR agonist without calcium effect is our ultimate goal.

In 1999, Boehm et al. reported the first nonsecosteroidal VDR agonist, LG190178 (**4**), and some groups since then have reported its derivatives.^{18–24} We focused on compound **4** as a new chemical class lead and conducted systematic SAR studies on the A part and the side chain of **4** to characterize the analogs, identifying carboxylic acid derivatives **5** and **6** as more potent nonsecosteroidal VDR agonists than 1,25(OH)₂D₃.^{25–27} From our X-ray analysis, we noted that a tight hydrogen-bonding network with VDR was made by the A part of **5** and **6**. However, these molecules have a lot of rotatable bonds in the A part, and gamma hydroxy carboxylic acid was easily cyclized to lactone in acidic conditions (Chart 1).

Then, by modeling based on X-ray conformation we attempted to optimize the A part again to reduce the flexibility and to avoid lactone formation by replacing the rotatable bonds with an aromatic ring. As a result, we identified a series of phenylacetic acid-type derivatives with very potent VDR agonistic activity. We

* Corresponding author. Tel.: +81 550 87 8626; fax: +81 550 87 5326.

E-mail address: kashiwagihrt@chugai-pharm.co.jp (H. Kashiwagi).

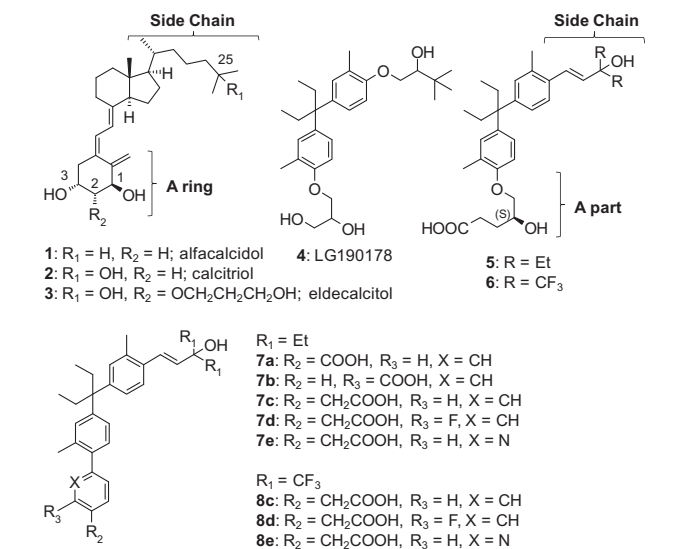
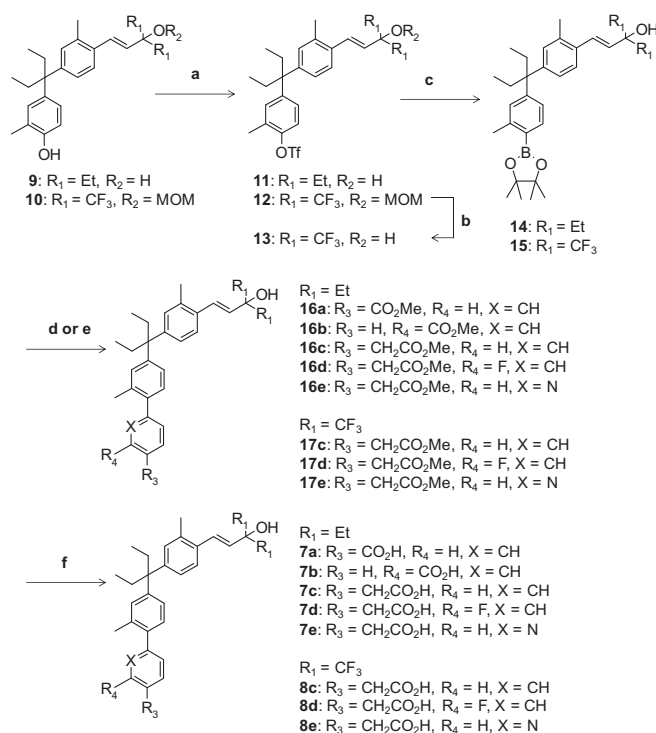


Chart 1. Structures of the secosteroids alfalcaldol (**1**), calcitriol (**2**), and eldecalcitol (**3**), and of the nonsecosteroidal analog LG190178 (**4**) and nonsecosteroidal carboxylic acid analogs (**5** to **7a–e** and **8c–e**). Parts labeled A of **5** and **6** (upper right) show the structural correspondence to the A ring of secosteroids (upper left).

also managed to combine the aryl acetic acid-type A parts and the (*E*)-olefin side chain with two terminal trifluoromethyl (CF₃) groups, which had shown the most potent *in vitro* activity in our previous study.²¹ As we expected, we found a series of potent VDR agonists. The structure of one of these compounds, **8d**, with VDR was solved by X-ray, and the detailed interactions of the A part and the side chain with VDR were confirmed. Furthermore, we evaluated the preventative effect of these compounds on BMD loss and serum calcium in an osteoporosis rat model using immature and mature rats. The pharmacokinetic parameters of **7e** were very good and it showed no signs of toxicity in a variety of safety tests both *in vitro* and *in vivo*. As a result, we identified compound **7e** (CH5036249) as the most promising clinical candidate.

2. Chemistry

The synthesis of compounds **7a–e** and **8c–e** is shown in Scheme 1. Compounds **9** and **10** were prepared by the method reported previously.²⁵ The treatment of phenols with bis(trifluoromethanesulfonyl)amide and triethylamine at rt afforded triflates **11** and **12** in excellent yield (98% and 99%, respectively). The methoxymethyl (MOM) group of **12** was deprotected with trifluoroacetic acid at rt in 99% yield. The triflates **11** and **13** were converted to boronates **14** and **15** with bis(pinacolato)diboron in the presence of palladium catalyst and potassium acetate at 110 °C in moderate yields. Suzuki coupling of these boronates and aryl bromides (methyl 3-bromobenzoate, methyl 4-bromobenzoate, methyl 4-bromophenylacetate) or aryl chloride (methyl 4-chloro-2-fluorophenylacetate) in the presence of palladium acetate with 2-dicyclohexylphosphino-2',6'-dimethoxy-1,1'-biphenyl (SPhos) ligand afforded biphenyl esters **16a–d** and **17c–d** in moderate to high yields. In the case of pyridine analogs, Suzuki coupling reactions of boronates **14** and **15** with methyl 2-(6-bromopyridin-3-yl)acetate were conducted at 110 °C using tetrakis(triphenylphosphine)palladium catalyst and gave biphenyl esters **16e** and **17e** in moderate yields (48% and 75%, respectively). These esters **16a–e** and **17c–e** were hydrolyzed to carboxylic acids **7a–e** and **8c–e** in moderate to high yields by treatment of 1 M sodium hydroxide solution and the following acidification process.



Scheme 1. Reagents and conditions: (a) PhN(Tf)₂, Et₃N, rt, CH₂Cl₂, 98–99%; (b) TFA, rt, CH₂Cl₂, 99%; (c) PdCl₂(dppf), dppf, bis(pinacolato)diboron, AcOK, 110 °C, 1,4-dioxane 65–90%; (d) aryl bromides or methyl 4-chloro-2-fluorophenylacetate, Pd(OAc)₂, SPhos, K₃PO₄, 100 °C, toluene–H₂O, 42–92%; (e) methyl 2-(6-bromopyridin-3-yl)acetate, Pd(PPh₃)₄, K₃PO₄, 110 °C, DMF, 48–75%; (f) 1 M NaOH, rt, THF–MeOH, 40–95%.

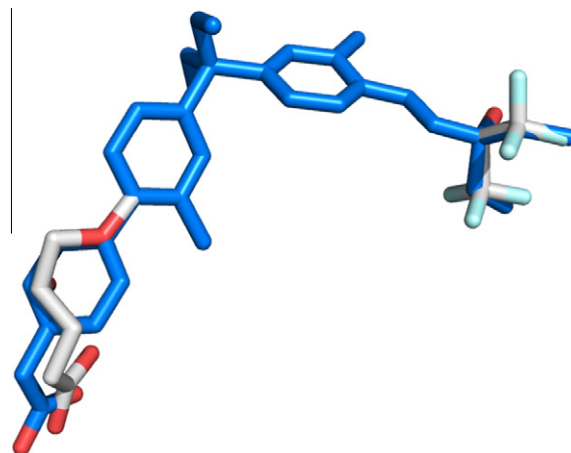


Figure 1. Superposition of modeled **7c** and **6** in the crystal (PDB ID: 3W0C). Compound **7c** is depicted in blue and compound **6** is depicted in white.

3. Results and discussion

All synthesized compounds were evaluated in MG-63 cells by reporter gene assay (RGA) (which contains vitamin D response element [VDRE] sequence derived from mouse osteopontin promoter) to measure vitamin D agonistic activity, and by osteocalcin production activity to measure the bone formation activity of the functional vitamin D agonistic effect. VDRE RGA activity and osteocalcin activity are represented by relative EC₅₀ values based on 1,25(OH)₂D₃ being assigned as 100% (a higher figure means stronger activity).^{25–27}

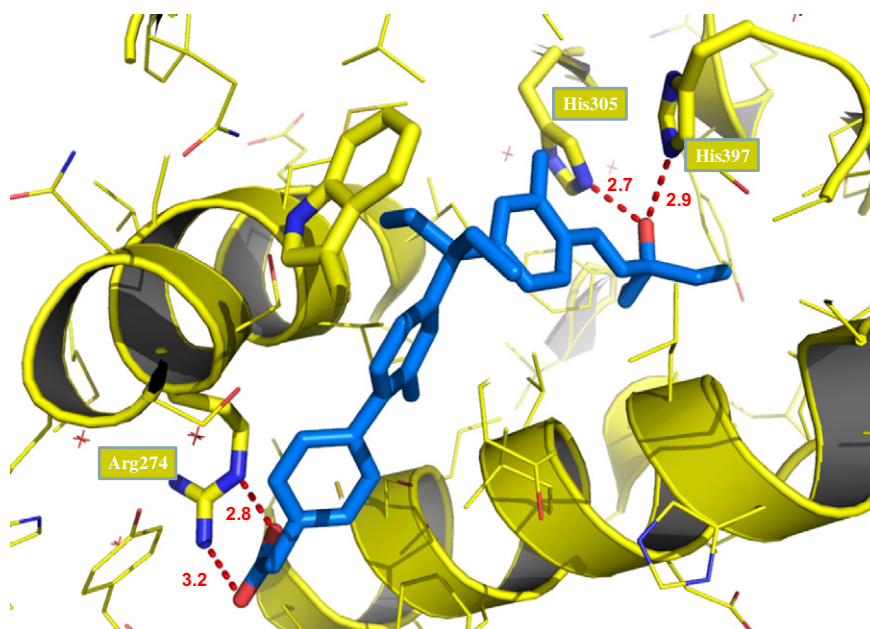
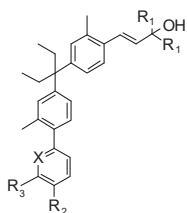


Figure 2. Model of compound **7c** in VDR. Key hydrogen bonding interactions are shown by red dotted lines and each distance is given in angstrom (Å).

Table 1
VDRE reporter gene and osteocalcin induction activity of carboxylic acid analogs in the A part

Compound	R ₁	R ₂	R ₃	X	VDRE RGA activity (%)	OC activity (%)
LG190178					6.7	185
1,25(OH) ₂ D ₃					100	100
5	Et				105	447
7a	Et	COOH	H	CH	5	12
7b	Et	H	COOH	CH	13	11
7c	Et	CH ₂ COOH	H	CH	89	1044
7d	Et	CH ₂ COOH	F	CH	112	508
7e	Et	CH ₂ COOH	H	N	89	652
6	CF ₃				592	3746
8c	CF ₃	CH ₂ COOH	H	CH	135	2233
8d	CF ₃	CH ₂ COOH	F	CH	116	1624
8e	CF ₃	CH ₂ COOH	H	N	121	1848



For compound **5** and **6** to exhibit potent VDR agonistic activity, it was very important for the carboxylic acid group to interact with Arg274 by forming a salt bridge. X-ray analysis of compound **6** with VDR showed that the methylene linker in the A part was folded like a ring without a linear form.²⁷ We focused on this folded conformation of the A-part moiety again and attempted to replace the methylene linker in the A part with a new phenyl ring to reduce flexibility. At the same time as inserting the new phenyl ring, we determined the optimal position of the carboxylic acid that binds to the ring.

Based on the crystallographic structure of compound **6** in complex with VDR (PDB ID: 3W0C), we constructed a docking model of the analog with a diethyl group in the side chain (Fig. 1). The compounds **7a–c** were manually docked into the crystal structure of VDR using software MOLOC.²⁸ These compounds were optimized using the MAB force field with a fixed VDR structure.

Figure 2 shows the result of modeling compound **7c**. In the model, the newly introduced phenyl ring (replacing the methylene linker in the A part of compound **6**) was beautifully adjusted in VDR without any steric repulsion to VDR protein. Next, to form the salt bridge interaction with Arg274 that was shown in compound **6**, the carboxylic acid group was introduced to the *para* position on the newly introduced phenyl ring with a methylene (**7c**). In our model, this carboxylic acid group was superposed excel-

lently with that of compound **6** and was expected to form a salt bridge with an ideal length (Figs. 1 and 2). The directly linked carboxylic acids on the phenyl ring at *para* or *meta* position (compounds **7a** and **7b**) were too far from Arg274 to form a salt bridge interaction in this model.

Table 1 shows all the *in vitro* results of compounds **7a–e** and **8c–e**. In benzoic acid analogs, those substituted at both the *meta* position **7a** and the *para* position **7b** showed very weak activity in the VDRE RGA and osteocalcin assays, as expected from the modeling with VDR. Because this activity was one-tenth of 1,25(OH)₂D₃, it seems these carboxylic acids could not form the salt bridge with Arg274. On the other hand, compound **7c**, which had an acetic acid at *para* position on the new phenyl ring, showed potent activity equivalent to 1,25(OH)₂D₃ in the VDRE reporter assay and, surprisingly, 10-fold more potent activity than 1,25(OH)₂D₃ in the osteocalcin induction assay. From these results, the carboxylic acid group of **7c** could form a good salt bridge with Arg274 in the same manner as that of **5** and accordingly we considered that the rigid 4-phenylacetic acid analog was completely mimicking the role of the folded carboxylic acid moiety in the A part of compound **5**. In our results, compound **7c** showed potent *in vitro* activity.

In a series of gamma hydroxy carboxylic acid analogs, the hydroxy group in the A-part had hydrogen-bonding interactions with

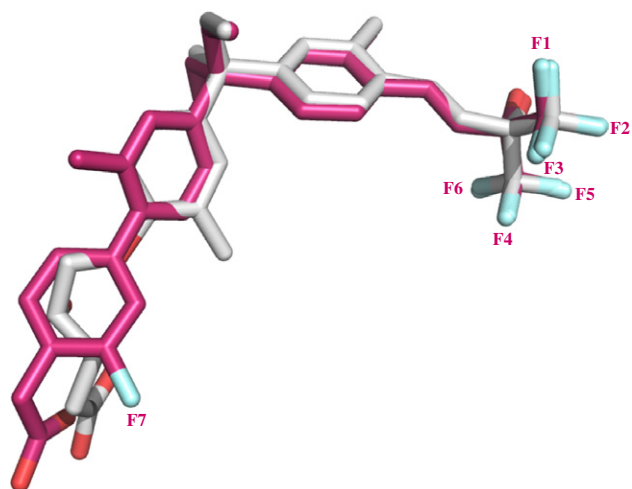


Figure 3. Superposition of binding conformations with VDR between compounds **8d** and **6** in the crystal (PDB ID: 3W0Y and 3W0C). Compound **8d** is depicted in magenta and compound **6** is depicted in white. All fluorine atoms in **8d** are labeled from F1 to F7.

Ser278 and Tyr143 of VDR and contributed to increasing the potency in vitro. To add an extra interaction with VDR to compound **7c**, such as the hydroxy group in compound **5**, we attempted to either introduce a fluorine atom at 3 position on the newly introduced phenyl ring or replace the phenyl ring with pyridine. As a result, fluorine analog **7d** showed more potent activity than $1,25(\text{OH})_2\text{D}_3$ and pyridine analog **7e** showed equivalent activity to $1,25(\text{OH})_2\text{D}_3$ in the VDRE assay. In the osteocalcin assay, compound **7d** showed fivefold and **7e** showed 6.5-fold more potent activity than $1,25(\text{OH})_2\text{D}_3$. Although these compounds had potent activity, they still had less than compound **7c**. We think compounds **7d** and **7e** were not gaining any additional hydrogen-bonding interactions, in spite of having the A part located in the hydrophilic pocket formed by Arg278, Tyr143, Ser278, Ser237, and crystal water.

In our previous report, a series of di- CF_3 analogs in the side chain moiety showed very potent VDR agonistic activity; especially (*E*)-olefin analog **6** was the most potent VDR agonist.²¹ We attempted to combine this potent side chain part with the newly found phenyl acetic acid moieties in the A part. As a result, phenyl acetic acid analog **8c** showed 1.35-fold more potent activity than $1,25(\text{OH})_2\text{D}_3$ in the VDRE assay, and 22-fold more potent activity in the osteocalcin assay. 3-Fluorophenyl acetic acid **8d** and pyridine acetic acid **8e** also showed more potent activity than $1,25(\text{OH})_2\text{D}_3$: respectively, 1.16-fold and 1.21-fold in VDRE RGA and 16-fold and 18-fold in the osteocalcin assay.

In the case of the A part of the gamma hydroxy carboxylic acid analog, an (*E*)-olefin side chain with terminal di- CF_3 group was very attractive for increasing VDR agonistic activity.

In detail, all six fluorine atoms had tight hydrophobic interactions with VDR residues; the two CF_3 electron-withdrawing groups increased the acidity of the hydroxy group in the side chain; the free rotation of the olefin linker was limited by the methyl group on the bisphenyl core; and the olefin itself was more hydrophobic than other linkers, which can be explained by the π constant. We think the total sum of these effects contributed to achieving the superagonistic activity seen in compound **6**, which was sixfold more potent than $1,25(\text{OH})_2\text{D}_3$ in the VDRE reporter assay and 37-fold more potent in the osteocalcin assay. Compared to diethyl analog **5**, di- CF_3 analog **6** was sixfold more potent in the VDRE reporter assay and eightfold more potent in the osteocalcin assay. However, with phenylacetic acid analogs in the A part, di- CF_3 ana-

log **8c** was only 1.5-fold more potent than diethyl analog **7c** in the VDRE reporter assay and twofold more potent in the osteocalcin assay. From these results, we realized that there is a distinct difference in the A part between these gamma hydroxy carboxylic acid analogs and the phenylacetic acid analogs, and that di- CF_3 analogs with phenylacetic acid analogs were weaker than we expected.

To confirm the detailed interactions of the phenylacetic acid group and CF_3 groups with VDR, we attempted to cocrystallize a human VDR ligand-binding domain with a series of our compounds, in accordance with a previously published method.^{25,27} From the crystallization screening, we obtained a cocrystal of **8d**/VDR. Figure 3 shows the superposition of the conformation of **8d** and **6** in each crystal. The side chain moieties of both compounds were completely superposed but some differences appeared in the A part. The carboxylic acid group in **8d** was slightly off the position of that in **6**, and the fluorine atom was located on the opposite side to that we expected. The methyl group on the bisphenyl core of the A part side in **8d** was also located on the opposite side to that in compound **6**.

Figure 4 shows the overall structure of compound **8d** which was consistent with that of compound **6**. The hydroxy group in the side chain moiety interacted with His305 and His397. The diethyl moiety between bisphenyl rings made a good $\text{CH}-\pi$ interaction with Trp278. It should be noted that the newly introduced phenyl ring in the A part fitted well, and the acetic acid moiety was placed near the targeted Arg274. However, instead of making a salt bridge with Arg274, this carboxylic acid interacted by hydrogen bondings with Arg274, two crystal waters and the backbone nitrogen of Asp144. The two crystal waters also made hydrogen bondings with Arg274 and Tyr236 in the same manner as reported (Fig. 5).²⁹ The newly introduced phenyl ring made a good $\pi-\pi$ interaction with Phe150. The fluorine atom in the A part, labeled F7, was placed on the opposite side to the hydroxy group of **6** and formed van der Waals (vdW) interactions with the $\text{C}\zeta$ and $\text{C}\epsilon$ atoms of Phe150 and the $\text{C}\delta$ and $\text{C}\epsilon$ atoms of Tyr236, and a weak electrostatic interaction with the hydroxy group of Ser237. This fluorine atom was also located close to (within 4 Å of) the carboxylic acid moiety, which may have contributed to fixing the conformation of this moiety by weak electrostatic interaction.

The fluorine interactions between the side chain and VDR were almost the same as previously reported.²⁷ All fluorine atoms (F1–F6) had many vdW contacts with hydrophobic residue of VDR as well as some electrostatic interactions. Within 4-Å-distance of each fluorine, a total of 29 contacts ($\text{CH}-\text{F}$ and $\text{NH}-\text{F}$ interactions) were observed.

In these results, phenylacetic acid derivatives showed equivalent or more potent activity than $1,25(\text{OH})_2\text{D}_3$. However, the SAR characteristics of these analogs were different from those of gamma hydroxy carboxylic acid analogs. Conformational analysis by X-ray of compounds **6** and **8d** showed that the side chain parts were completely superposed, the hydroxy group had hydrogen bonding with two histidines, and the pattern of interactions of six fluorines with hydrophobic amino acids was the same. On the other hand, the newly introduced phenyl ring mimicked well the folded methylene linker in the A part of compound **6**, even though the position of the carboxylic acid group was not superposed completely. Consequently, the carboxylic acid of compound **8d** formed hydrogen-bonding interactions with Arg274 and crystal water instead of making the salt bridge interaction. Furthermore, phenylacetic acid analogs did not have a substituent corresponding to the hydroxy group in the A part of compound **5** or **6** that interacted with Ser278 and Tyr143 by hydrogen bonding. This interaction corresponded to the hydroxy group of 3-position of $1,25(\text{OH})_2\text{D}_3$, and the lack of it could have resulted in a different chemical class from the series of gamma hydroxy carboxylic acid analogs and would therefore produce a different SAR.

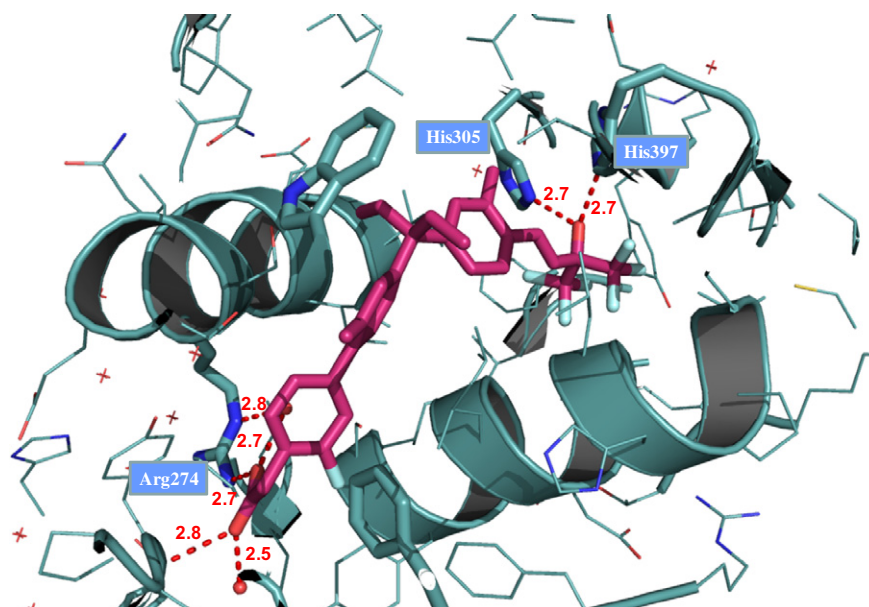


Figure 4. Overall X-ray crystal structure of compound **8d** (magenta) bound to VDR (cyan). Key hydrogen bonding interactions are shown by red dotted lines and each distance is given in Å (PDB ID: 3W0Y).

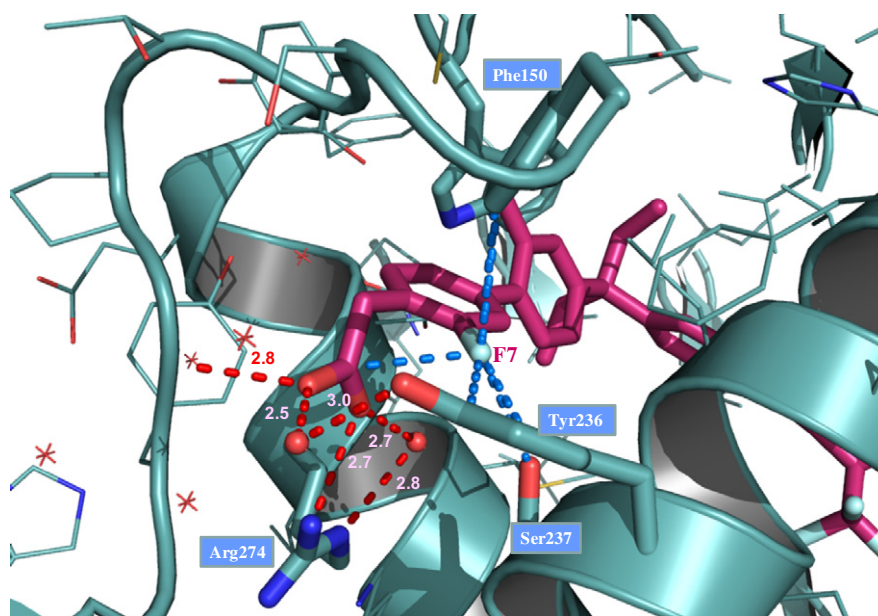


Figure 5. Detailed hydrogen bonding network and fluorine interactions around the A part of compound **8d** (magenta) bound to VDR (cyan). Key hydrogen-bonding interactions are shown by red dotted lines and each distance is given in Å. Fluorine contacts within 4 Å of VDR residue atoms are shown by blue dotted lines. The fluorine atom is labeled F7 (PDB ID: 3W0Y).

Next, we evaluated the potency of a series of compounds (**7c**, **7e**, **8c**, and **8d**) in vivo using immature, osteoporosis rats (Table 2). Female, 8-week-old, Sprague–Dawley rats were either ovariectomized (OVX) to produce the estrogen-deficient condition observed in postmenopausal women that promotes BMD loss, or sham-operated. The compounds (25 and 50 ng/kg of **7c**, 10, 20 and 40 ng/kg of **7e**, 10 and 30 ng/kg of **8c**, and 20 and 60 ng/kg of **8d**, per day) were orally administered to OVX rats while only vehicle was administered to the OVX-control and sham-operated groups. These doses were determined from the serum calcium level after 4-day treatment of normal rats by po administration of three dosages of each compound. The dose at which around 11 mg/dL of serum calcium level was observed was selected as the higher dose of this study

(data not shown). After five times per week administration for 4 weeks, BMD in the distal femur was measured by dual-energy X-ray absorptiometry. Compound **7c** dose-dependently prevented BMD loss in osteoporosis rats, and the ratio to the vehicle group was 42% at 25 ng/kg and 81% at 50 ng/kg. Normal serum calcium level was maintained at the 25 ng/kg dosage but a rise in the level of calcium was observed in the 50 ng/kg dosing group. Compound **7e** not only prevented BMD loss, but also increased BMD, with the ratios to the vehicle group of 122% at 10 ng/kg, 172% at 20 ng/kg, and 198% at 40 ng/kg. In the 10 and 20 ng/kg groups, serum calcium elevation was not observed but in the 40 ng/kg group, a clear calcium elevation was observed. Compounds **8c** and **8d** also showed dose-dependent BMD loss prevention at 10 and 30 ng/kg,

Table 2
Oral once-daily treatment for 4 weeks prevented BMD loss in eight-week-old osteoporosis model rats

Compound	Dose (ng/kg)	Sham	Femoral distal BMD (mg/cm ²)			Serum Ca (mg/dL)		
			Vehicle	Treated	ΔBMD ^a (%)	Vehicle	Treated	ΔCa ^b (%)
1,25(OH) ₂ D ₃	20	166.1 ± 2.6*	133.6 ± 5.2	134.9 ± 2.7	4	9.82 ± 0.12	10.07 ± 0.14	2.5
	80			150.9 ± 4.3*	53		10.07 ± 0.05	2.5
	320			152.3 ± 3.7*	58		10.32 ± 0.12 [†]	5.1
7c	25	162.9 ± 4.0*	138.6 ± 1.3	148.7 ± 2.2 [†]	42	10.30 ± 0.18	10.37 ± 0.08	0.7
	50			158.2 ± 2.2 [†]	81		11.20 ± 0.12 [†]	8.7
7e	10	141.5 ± 3.9 [#]	131.6 ± 2.7	143.7 ± 3.3 [†]	122	10.27 ± 0.15	9.97 ± 0.16	-2.9
	20			148.6 ± 4.0 [†]	172		10.50 ± 0.17	2.2
	40			151.3 ± 2.2 [†]	198		11.13 ± 0.24 [†]	8.4
8c	10	159.1 ± 2.5*	139.4 ± 3.0	148.6 ± 3.1	47	10.27 ± 0.08	10.33 ± 0.16	0.6
	30			157.0 ± 2.5 [†]	89		10.98 ± 0.21 [†]	6.9
8e	20	159.1 ± 2.5*	139.4 ± 3.0	144.4 ± 3.1	25	10.27 ± 0.08	10.58 ± 0.07 [†]	3.0
	60			150.3 ± 3.3 [†]	55		11.32 ± 0.15 [†]	10.2

All data show mean value ± SE (n = 6).

* p < 0.05 versus vehicle.

[#] p = 0.06 versus vehicle.

^a ΔBMD was calculated as follows: (treated BMD–vehicle BMD)/(sham BMD–vehicle BMD) × 100 (%).

^b ΔCa was calculated as follows: (treated Ca–vehicle Ca)/(vehicle Ca) × 100 (%).

Table 3
Pharmacokinetic parameters of 7e after intravenous and oral administration at 100 μg/kg in rats (n = 3)

	iv	po
F (%)		95.1
T _{1/2}	8.5 ± 1.4	17.6 ± 3.3
C _{max} (ng/mL)		54.0 ± 8.2
AUC _{inf} (ng/mL·h)	1128 ± 203	1648 ± 195
MRT (h)	11.2 ± 2.2	28.3 ± 4.7
V _{ss} (mL/kg)	990 ± 16	
CLt (mL/h/kg)	90.6 ± 16.2	

and at 20 and 60 ng/kg respectively. Lower dose groups showed the normal range of serum calcium level; however, in higher dose groups, a rise in serum calcium was observed for both compounds **8c** and **8d**. From these results, we confirmed the effect of preventing BMD loss in all the tested compounds in osteoporosis rats. Especially in lower dosing groups, all compounds showed moderate to potent effect while maintaining serum calcium in the normal range. Surprisingly, the BMD levels of compound **7e** at the doses of 10 and 20 ng/kg were higher than those of the sham group, without raising the serum calcium. This *in vivo* efficacy of **7e** was clearly more potent than that of 1,25(OH)₂D₃.

From the efficacy in the osteoporosis model using immature rats and the pharmacokinetic profiles, we selected the pyridine derivative **7e** for further evaluation. Table 3 shows the pharmacokinetic parameters in male rat at the single dosage of 100 μg/kg via intravenous and oral administration. Compound **7e** shows excellent bioavailability (F = 95%), a favorable half-life (T_{1/2} = 17.6 h), a long mean residence time (MRT = 28.3 h), and small total clearance (CLt = 91 mL/h/kg).

Using 8-week-old rats of the osteoporosis model was very convenient for screening the compounds, but in immature rats the effect of preventing BMD loss in an estrogen-deficient condition may have been affected by an increase in BMD caused by bone formation due to normal growth. To confirm the ability to prevent BMD loss without including bone formed by normal growth, we evaluated the same osteoporosis model using 8-month-old rats. We consider the osteoporosis shown in post menopausal women is better reflected by the mature rats of this osteoporosis model than by immature ones.

Using 8-week-old rats of the osteoporosis model was very convenient for screening the compounds, but in immature rats the effect of preventing BMD loss in an estrogen-deficient condition may have been affected by an increase in BMD caused by bone forma-

tion due to normal growth. To confirm the ability to prevent BMD loss without including bone formed by normal growth, we evaluated the same osteoporosis model using 8-month-old rats. We consider the osteoporosis shown in post menopausal women is better reflected by the mature rats of this osteoporosis model than by immature ones.

We evaluated the potency of **7e** in mature rats of the osteoporosis model (Fig. 6). Compound **7e** was orally administered to five groups (0.75, 1.5, 3.0, 6.0 and 12 ng/kg per day) of female, 8-month-old, Sprague–Dawley rats, and vehicle was administered to the OVX-control and sham-operated groups. After administration five times per week for 4 weeks, BMD in the distal femur and lumbar spine was measured. BMD in the OVX-control group was significantly reduced compared with the sham-operated group. In rats in which osteoporosis had been caused by ovariectomy, compound **7e** dose-dependently prevented BMD loss in both distal femur and lumbar spine without body weight loss. Normal serum calcium level was maintained at the doses of 0.75–6.0 ng/kg; however, in the highest (12 ng/kg) dosing group, a rise in calcium level was observed.

Compound **7e** was not the most potent one *in vitro*; however it showed potent BMD effect *in vivo*. When speculating upon this discrepancy, we noted that VDR agonists relate strongly to both bone formation and bone resorption. Because we only evaluated bone formation as one of the functional VDR agonistic effects by looking at osteocalcin induction activity, we did not evaluate whether **7e** suppressive effect on bone resorption³⁰ was more potent than other compounds. Further evaluation will explain the discrepancy between *in vivo* and *in vitro* effects of **7e** on bone.

In further safety assessment, compound **7e** (CH5036249) showed negative results on the micro-AMES and micronucleus tests *in vitro*, and also showed no concerns of toxicity except for hypercalcemia in a 4-week repeated administration to normal rats at the higher dosage of 108 ng/kg *in vivo*. CYP induction ability of compound **7e** at 10 nM concentration was negative for CYP1A and weaker than 1,25(OH)₂D₃ for CYP3A.³¹ We consider our nonsteroidal VDR agonist CH5036249 to be a possible new drug candidate for the treatment of osteoporosis in human.

4. Conclusion

A series of nonsteroidal VDR agonists were explored in an extension of our study of gamma hydroxy carboxylic acid analogs. They have aryl acetic acid instead of 1,3-diol of 1,25(OH)₂D₃ and showed more potent activity *in vitro* than

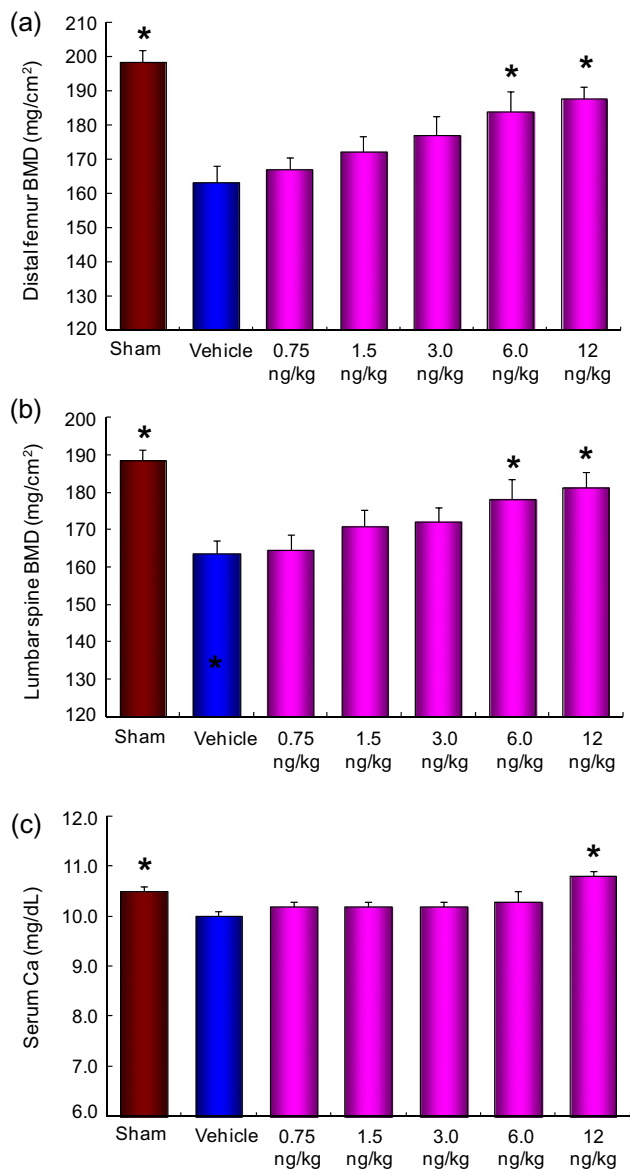


Figure 6. Oral once-daily treatment of compound **7e** prevented BMD loss in distal femur (a) and lumbar spine (b) in 8-month-old osteoporosis model rats. (c) Serum calcium concentration in osteoporosis model rats. All data are the mean value \pm SE ($n = 8$). * $p < 0.05$ versus vehicle.

1,25(OH)₂D₃. An X-ray analysis of **8d** showed that the substituting phenyl ring mimicked well the folded methylene linker of gamma hydroxy carboxylic acid moiety but the carboxylic acid of **8d** interacted with VDR in a different pattern from the one in gamma hydroxy carboxylic acids. Through our in vivo screening using immature rats of an osteoporosis model, a potent active vitamin D₃ analog, compound **7e**, was identified. Compound **7e** also showed excellent ability to prevent BMD loss in mature rats of the osteoporosis model, without severe hypercalcemia and with good PK profiling. Our nonsteroidal VDR agonist **7e** (CH5036249) could be a possible new drug candidate for the treatment of osteoporosis in humans.

5. Experimental

5.1. Chemistry: general

Purchased reagents and solvents were used without further purification unless otherwise noted. ¹H and ¹³C NMR spectra

were carried out on VARIAN 400-MR spectrophotometers; chemical shifts are reported in parts per million (ppm) downfield from that of internal tetramethylsilane (TMS). Mass spectrophotometry was measured with a Waters ACQUITY SQD electrospray ionization (ESI) system. High-resolution mass spectra (HRMS) were recorded on Thermo Fisher Scientific LTQ Orbitrap XL (ESI) instruments. Chromatographic purification was carried out using Merck silica gel 60 (column) or Merck silica gel 60 PF₂₅₄ (preparative TLC).

5.1.1. Trifluoromethanesulfonic acid 4-{1-Ethyl-1-[4-((E)-3-ethyl-3-hydroxy-1-pentenyl)-3-methylphenyl]propyl}-2-methylphenyl ester (**11**)

To a solution of **9** (100 mg, 0.263 mmol) in CH₂Cl₂ (3 mL) were added *N*-phenylbis(trifluoromethanesulfonimide) (122 mg, 0.342 mmol) and Et₃N (0.072 mL, 0.526 mmol), and the mixture was stirred at rt overnight. The mixture was concentrated and the obtained residue was purified by preparative TLC (*n*-hexane/AcOEt = 4:1) to afford **11** (132 mg, 98%) as colorless oil. ¹H NMR (CDCl₃) δ : 0.62 (6H, t, $J = 7.2$ Hz), 0.92 (6H, t, $J = 7.4$ Hz), 1.64 (4H, q, $J = 7.4$ Hz), 2.08 (4H, q, $J = 7.2$ Hz), 2.32 (6H, s), 6.03 (1H, d, $J = 16.0$ Hz), 6.76 (1H, d, $J = 16.0$ Hz), 6.90–6.94 (2H, m), 7.05 (1H, dd, $J = 8.7, 1.9$ Hz), 7.09–7.12 (2H, m), 7.32 (1H, d, $J = 7.8$ Hz). ¹³C NMR (CDCl₃) δ : 149.1, 146.6, 146.2, 136.2, 134.7, 133.8, 131.6, 129.7, 129.5, 129.4, 127.3, 125.8, 125.7, 125.0, 120.2, 76.0, 49.3, 33.2, 29.0, 20.1, 16.5, 8.3, 7.8. MS (ESI positive): 535 (M+Na)⁺.

5.1.2. Trifluoromethanesulfonic acid 4-{1-ethyl-1-[3-methyl-4-((E)-4,4,4-trifluoro-3-methoxymethoxy-3-trifluoromethyl-1-butenyl)phenyl] propyl}-2-methylphenyl ester (**12**)

The yield was 99%. Colorless oil. ¹H NMR (CDCl₃) δ : 0.62 (6H, t, $J = 7.2$ Hz), 2.08 (4H, q, $J = 7.2$ Hz), 2.32 (6H, s), 3.51 (3H, s), 4.97 (2H, s), 6.08 (1H, d, $J = 16.6$ Hz), 6.96–7.00 (2H, m), 7.01–7.08 (2H, m), 7.11 (1H, d, $J = 8.4$ Hz), 7.33–7.38 (2H, m). ¹³C NMR (CDCl₃) δ : 149.2, 148.7, 146.4, 137.6, 135.9, 131.6, 130.1, 129.8, 127.3, 126.2, 125.5, 123.8, 121.0, 120.4, 120.2, 117.0, 115.2, 93.3, 56.4, 49.6, 29.0, 19.9, 16.6, 8.3. MS (ESI positive): 654 (M+NH₄)⁺.

5.1.3. Trifluoromethanesulfonic acid 4-{1-Ethyl-1-[3-methyl-4-((E)-4,4,4-trifluoro-3-hydroxy-3-trifluoromethyl-1-butenyl)phenyl] propyl}-2-methylphenyl ester (**13**)

To a solution of **12** (2.41 g, 3.79 mmol) in CH₂Cl₂ (20 mL) was added trifluoroacetic acid (2.0 mL) and the mixture was stirred at rt for 30 min. The reaction mixture was concentrated and purified with silicagel chromatography (*n*-hexane/AcOEt = 100:0 to 70:30) to give **13** (2.24 g, 99%) as a colorless oil. ¹H NMR (CDCl₃) δ : 0.62 (6H, t, $J = 7.1$ Hz), 2.10 (4H, q, $J = 7.1$ Hz), 2.32 (3H, s), 2.35 (3H, s), 6.12 (1H, d, $J = 15.8$ Hz), 6.96–7.00 (2H, m), 7.05 (1H, dd, $J = 8.6, 2.2$ Hz), 7.09 (1H, s), 7.12 (1H, d, $J = 8.6$ Hz), 7.37 (1H, d, $J = 8.8$ Hz), 7.41 (1H, d, $J = 15.8$ Hz). ¹³C NMR (CDCl₃) δ : 148.9, 148.8, 146.4, 135.8, 135.0, 131.7, 131.4, 130.1, 129.8, 127.3, 126.1, 125.6, 123.9, 121.1, 120.3, 120.2, 117.1, 49.5, 29.0, 19.9, 16.5, 8.2. MS (ESI positive): 593 (M+H)⁺.

5.1.4. (E)-3-Ethyl-1-(4-{1-ethyl-1-[3-methyl-4-(4,4,5,5-tetramethyl-[1,3,2]dioxaborolan-2-yl) phenyl] propyl}-2-methylphenyl)-1-penten-3-ol (**14**)

To a solution of **11** (1.6 g, 3.1 mmol) in 1,4-dioxane (20 mL) were added 1,1'-Bis(diphenylphosphino)-ferrocene (dppf) (104 mg, 0.19 mmol), KOAc (0.919 g, 9.4 mmol), Bis(pinacolato)diboron (1.03 g, 4.1 mmol), and [1,1-bis(diphenylphosphino)-ferrocene]dichloropalladium(II) (PdCl₂dppf), complex with CH₂Cl₂ (1:1) (0.15 g, 0.19 mmol). The mixture was stirred at 80 °C overnight under nitrogen atmosphere. The mixture was poured into H₂O and products were extracted with CH₂Cl₂. The extracts were dried over anhydrous MgSO₄ and concentrated. The obtained residue was chromatographed on silica gel (*n*-hexane/AcOEt = 10:1) to afford **14** (1.0 g, 65%) as a colorless oil. ¹H NMR (CDCl₃)

δ : 0.60 (6H, t, $J = 7.3$ Hz), 0.91 (6H, t, $J = 7.3$ Hz), 1.32 (12H, s), 1.63 (4H, q, $J = 7.3$ Hz), 2.08 (4H, q, $J = 7.3$ Hz), 2.29 (3H, s), 2.48 (3H, s), 6.01 (1H, d, $J = 15.8$ Hz), 6.74 (1H, d, $J = 16.0$ Hz), 6.91–7.01 (4H, m), 7.28 (1H, d, $J = 8.2$ Hz), 7.64 (1H, d, $J = 7.6$ Hz). ^{13}C NMR (CDCl_3) δ : 151.4, 147.5, 144.0, 135.8, 135.2, 134.4, 133.3, 130.0, 129.6, 125.9, 125.9, 124.8, 124.7, 83.2, 75.9, 49.6, 33.3, 29.0, 24.9, 22.5, 20.2, 8.4, 7.9. MS (ESI positive): 508 (M+H) $^+$.

5.1.5. (*E*)-4-(4-{1-Ethyl-1-[3-methyl-4-(4,4,5-tetramethyl-1,3,2)dioxaborolan-2-yl]phenyl}propyl)-2-methylphenyl-1,1,1-trifluoro-2-trifluoromethyl-3-buten-2-ol (15)

The yield was 90%. Colorless oil. ^1H NMR (CDCl_3) δ : 0.61 (6H, t, $J = 7.2$ Hz), 1.32 (12H, s), 2.09 (4H, q, $J = 7.2$ Hz), 2.31 (3H, s), 2.48 (3H, s), 6.08 (1H, d, $J = 16.0$ Hz), 6.93–7.02 (4H, m), 7.33 (1H, d, $J = 7.6$ Hz), 7.38 (1H, d, $J = 16.4$ Hz), 7.64 (1H, d, $J = 7.6$ Hz). ^{13}C NMR (CDCl_3) δ : 151.0, 149.8, 144.1, 135.5, 135.3, 135.1, 130.9, 130.3, 130.2, 129.6, 128.7, 126.2, 126.2, 125.3, 125.2, 124.6, 116.6, 83.3, 49.8, 28.9, 24.8, 22.5, 19.9, 8.3. MS (ESI positive): 588 (M+NH $_4$) $^+$.

5.1.6. General procedure for Suzuki coupling reaction of boronate 14 and 15

To a solution of boronate (0.037 mmol) in toluene (1.5 mL) and H $_2$ O (0.15 mL) were added arylhalide (methyl 3-bromobenzoate, methyl 4-bromobenzoate, methyl (4-bromophenyl)-acetate, or methyl (4-chloro-2-fluorophenyl)-acetate) (0.055 mmol), Pd(OAc) $_2$ (0.8 mg, 0.0037 mmol), 2-dicyclohexylphosphino-2',6'-dimethoxy-1,1'-biphenyl (SPhos) (3.0 mg, 0.0073 mmol), and K $_3$ PO $_4$ (23 mg, 0.110 mmol) and the mixture was stirred at 100 $^\circ\text{C}$ for 1.5 h under nitrogen atmosphere. The mixture was poured into satd NaHCO $_3$ aq solution and the products were extracted with CH $_2$ Cl $_2$. The extracts were dried over anhydrous MgSO $_4$ and concentrated. The obtained residue was purified by preparative TLC (*n*-hexane/AcOEt = 4:1) to give ester.

5.1.7. 4'-{1-Ethyl-1-[4-((*E*)-3-ethyl-3-hydroxy-1-pentenyl)-3-methylphenyl]propyl}-2'-methylbiphenyl-4-carboxylic acid methyl ester (16a)

The yield was 67%. Colorless oil. ^1H NMR (CDCl_3) δ : 0.66 (6H, t, $J = 7.2$ Hz), 0.92 (6H, t, $J = 7.5$ Hz), 1.65 (4H, q, $J = 7.5$ Hz), 2.13 (4H, q, $J = 7.3$ Hz), 2.23 (3H, s), 2.34 (3H, s), 3.94 (3H, s), 6.03 (1H, d, $J = 15.9$ Hz), 6.76 (1H, d, $J = 15.9$ Hz), 6.96–7.02 (6H, m), 7.05 (1H, dd, $J = 7.7$, 2.1 Hz), 7.08–7.12 (3H, m), 7.33 (1H, d, $J = 7.8$ Hz), 7.41 (2H, d, $J = 8.6$ Hz), 8.07 (2H, d, $J = 8.6$ Hz). ^{13}C NMR (CDCl_3) δ : 167.2, 148.2, 147.5, 146.9, 137.7, 135.9, 134.5, 134.0, 133.4, 130.1, 129.9, 129.5, 129.4, 129.3, 128.9, 126.0, 125.9, 125.8, 124.9, 76.0, 52.1, 49.4, 33.3, 29.1, 20.7, 20.3, 8.5, 7.9. MS (ESI negative): 497 (M–H) $^-$.

5.1.8. 4'-{1-Ethyl-1-[4-((*E*)-3-ethyl-3-hydroxy-1-pentenyl)-3-methylphenyl]propyl}-2'-methylbiphenyl-3-carboxylic acid methyl ester (16b)

The yield was 51%. Colorless oil. ^1H NMR (CDCl_3) δ : 0.67 (6H, t, $J = 7.3$ Hz), 0.93 (6H, t, $J = 7.5$ Hz), 1.65 (4H, q, $J = 7.5$ Hz), 2.13 (4H, q, $J = 7.3$ Hz), 2.22 (3H, s), 2.34 (3H, s), 3.92 (3H, s), 6.03 (1H, d, $J = 15.9$ Hz), 6.77 (1H, d, $J = 15.9$ Hz), 6.98–7.02 (2H, m), 7.05 (1H, dd, $J = 7.9$, 1.8 Hz), 7.08–7.11 (2H, m), 7.33 (1H, d, $J = 8.1$ Hz), 7.46 (1H, t, $J = 7.7$ Hz), 7.53 (1H, d, $J = 7.6$ Hz), 7.99 (1H, d, $J = 7.6$ Hz), 8.02 (1H, s). ^{13}C NMR (CDCl_3) δ : 167.2, 148.0, 147.6, 142.2, 137.7, 135.9, 134.5, 134.1, 133.8, 133.4, 130.5, 130.0, 129.9, 129.6, 129.0, 128.1, 127.7, 126.0, 125.9, 125.8, 124.9, 76.0, 52.1, 49.3, 33.3, 29.1, 20.7, 20.3, 8.5, 7.9. MS (ESI positive): 521 (M+H) $^+$.

5.1.9. 4'-{1-Ethyl-1-[4-((*E*)-3-ethyl-3-hydroxy-1-pentenyl)-3-methylphenyl]propyl}-2'-methylbiphenyl-4-yl)acetic acid methyl ester (16c)

The yield was 42%. Colorless oil. ^1H NMR (CDCl_3) δ : 0.66 (6H, t, $J = 7.2$ Hz), 0.92 (6H, t, $J = 7.5$ Hz), 1.65 (4H, q, $J = 7.5$ Hz), 2.12 (4H,

q, $J = 7.3$ Hz), 2.23 (3H, s), 2.34 (3H, s), 3.67 (2H, s), 3.73 (3H, s), 6.03 (1H, d, $J = 15.9$ Hz), 6.76 (1H, d, $J = 15.9$ Hz), 6.97–7.03 (3H, m), 7.05–7.10 (2H, m), 7.30 (4H, s), 7.33 (1H, d, $J = 8.1$ Hz). ^{13}C NMR (CDCl_3) δ : 172.2, 147.6, 147.5, 140.8, 138.3, 135.9, 134.4, 134.1, 133.3, 132.1, 129.9, 129.5, 129.1, 128.8, 126.0, 125.9, 125.7, 124.9, 76.0, 52.1, 49.3, 40.9, 33.3, 29.1, 20.8, 20.3, 8.5, 7.9. MS (ESI negative): 511 (M–H) $^-$.

5.1.10. 4'-{1-Ethyl-1-[4-((*E*)-3-ethyl-3-hydroxy-1-pentenyl)-3-methylphenyl]propyl}-3-fluoro-2'-methylbiphenyl-4-yl)acetic acid methyl ester (16d)

The yield was 76%. Colorless oil. ^1H NMR (CDCl_3) δ : 0.65 (6H, t, $J = 7.1$ Hz), 0.92 (6H, t, $J = 7.4$ Hz), 1.64 (4H, q, $J = 7.4$ Hz), 2.11 (4H, q, $J = 7.0$ Hz), 2.24 (3H, s), 2.34 (3H, s), 3.71 (2H, s), 3.74 (3H, s), 6.03 (1H, d, $J = 16.0$ Hz), 6.76 (1H, d, $J = 16.0$ Hz), 6.97–7.09 (7H, m), 7.28 (1H, d, $J = 7.4$ Hz), 7.33 (1H, d, $J = 8.0$ Hz). ^{13}C NMR (CDCl_3) δ : 171.3, 159.3, 148.0, 147.5, 143.3, 137.3, 135.9, 134.5, 134.1, 130.8, 130.0, 129.9, 128.9, 126.0, 125.8, 125.7, 125.2, 125.1, 124.9, 119.2, 116.4, 76.0, 52.2, 49.3, 34.1, 33.3, 29.1, 20.8, 20.3, 8.5, 7.9. MS (ESI negative): 529 (M–H) $^-$.

5.1.11. 4'-{1-Ethyl-1-[3-methyl-4-((*E*)-4,4,4-trifluoro-3-hydroxy-3-trifluoromethyl-1-butenyl)phenyl]propyl}-2'-methylbiphenyl-4-yl)acetic acid methyl ester (17c)

The yield was 92%. Colorless oil. ^1H NMR (CDCl_3) δ : 0.66 (6H, t, $J = 7.3$ Hz), 2.13 (4H, q, $J = 7.2$ Hz), 2.22 (3H, s), 2.34 (3H, s), 3.66 (2H, s), 3.71 (3H, s), 6.10 (1H, d, $J = 16.1$ Hz), 7.00 (1H, dd, $J = 8.1$, 1.7 Hz), 7.03–7.10 (4H, m), 7.29 (4H, d, $J = 2.0$ Hz), 7.36 (1H, d, $J = 8.8$ Hz), 7.39 (1H, d, $J = 15.6$ Hz). ^{13}C NMR (CDCl_3) δ : 172.2, 149.9, 147.1, 140.7, 138.5, 135.5, 134.3, 132.8, 132.1, 130.9, 130.2, 129.9, 129.5, 129.1, 128.8, 126.3, 125.6, 125.4, 121.2, 116.5, 52.1, 49.5, 40.8, 29.0, 20.8, 20.0, 8.4. MS (ESI negative): 591 (M–H) $^-$.

5.1.12. 4'-{1-Ethyl-1-[3-methyl-4-((*E*)-4,4,4-trifluoro-3-hydroxy-3-trifluoromethyl-1-butenyl)phenyl]propyl}-3-fluoro-2'-methylbiphenyl-4-yl)acetic acid methyl ester (17d)

The yield was 61%. Colorless oil. ^1H NMR (CDCl_3) δ : 0.65 (6H, t, $J = 7.2$ Hz), 2.12 (4H, q, $J = 7.2$ Hz), 2.23 (3H, s), 2.36 (3H, s), 3.71 (2H, s), 3.74 (3H, s), 6.10 (1H, d, $J = 15.8$ Hz), 6.99–7.09 (7H, m), 7.28 (1H, d, $J = 7.8$ Hz), 7.37 (1H, d, $J = 8.4$ Hz), 7.39 (1H, d, $J = 16.0$ Hz). ^{13}C NMR (CDCl_3) δ : 171.4, 159.3, 149.9, 147.7, 143.3, 143.2, 137.4, 135.6, 135.1, 134.2, 130.9, 130.8, 130.2, 130.0, 129.0, 126.3, 125.7, 125.5, 125.1, 125.1, 119.4, 116.4, 116.4, 52.3, 49.5, 34.1, 29.0, 20.8, 20.0, 8.4. MS (ESI negative): 609 (M–H) $^-$.

5.1.13. [6-(4-{1-Ethyl-1-[4-((*E*)-3-ethyl-3-hydroxy-1-pentenyl)-3-methylphenyl]propyl}-2-methylphenyl)pyridin-3-yl]acetic acid methyl ester (16e)

To a solution of **14** (50 mg, 0.102 mmol) in DMF (1 mL) were added methyl 2-(6-bromopyridin-3-yl)acetate (38.0 mg, 0.165 mmol), tetrakis(triphenylphosphine)palladium(0) (23.1 mg, 0.020 mmol), and K $_3$ PO $_4$ (63.9 mg, 0.301 mmol). The mixture was stirred at 110 $^\circ\text{C}$ for 30 min under nitrogen atmosphere. The mixture was poured into satd NaHCO $_3$ aq solution and the products were extracted with AcOEt. The extracts were washed with water and brine, dried over anhydrous MgSO $_4$ and concentrated. The obtained residue was purified by preparative TLC (*n*-hexane/AcOEt = 2:1) to give **16e** (24.6 mg, 48%) as a colorless oil. ^1H NMR (CDCl_3) δ : 0.65 (6H, t, $J = 7.2$ Hz), 0.92 (6H, t, $J = 7.4$ Hz), 1.64 (4H, q, $J = 7.4$ Hz), 2.11 (4H, q, $J = 7.0$ Hz), 2.32 (3H, s), 2.32 (3H, s), 3.68 (2H, s), 3.75 (3H, s), 6.02 (1H, d, $J = 16.0$ Hz), 6.75 (1H, d, $J = 16.0$ Hz), 6.96–7.01 (2H, m), 7.05–7.10 (2H, m), 7.27 (1H, d, $J = 7.0$ Hz), 7.31 (1H, d, $J = 7.8$ Hz), 7.39 (1H, d, $J = 8.2$ Hz), 7.69 (1H, dd, $J = 8.0$, 2.2 Hz), 8.57 (1H, s). ^{13}C NMR (CDCl_3) δ : 171.4, 159.0, 149.6, 148.7, 147.6, 137.0, 136.9, 135.9, 134.8, 134.5, 133.4, 130.5, 130.1, 129.0, 127.2, 126.0, 125.9, 124.8, 123.8, 76.0,

52.3, 49.4, 38.0, 33.3, 29.1, 20.6, 20.3, 8.4, 7.9. MS (ESI positive): 514 (M+H)⁺.

5.1.14. [6-(4-{1-Ethyl-1-[3-methyl-4-((E)-4,4,4-trifluoro-3-hydroxy-3-trifluoromethyl-1-butenyl]phenyl)propyl]-2-methylphenyl}pyridin-3-yl)acetic acid methyl ester (17e)

The yield was 75%. Colorless oil. ¹H NMR (CDCl₃) δ: 0.64 (6H, t, J = 7.1 Hz), 2.11 (4H, q, J = 7.0 Hz), 2.28 (3H, s), 2.28 (3H, s), 3.60 (2H, s), 3.72 (3H, s), 6.05 (1H, d, J = 16.2 Hz), 6.98–7.06 (4H, m), 7.23 (1H, dd, J = 8.0, 2.2 Hz), 7.30 (1H, dd, J = 8.0, 3.3 Hz), 7.36 (1H, d, J = 16.2 Hz), 7.38 (1H, d, J = 7.8 Hz), 7.70 (1H, d, J = 7.6 Hz), 8.54 (1H, s). ¹³C NMR (CDCl₃) δ: 171.3, 158.7, 150.5, 150.0, 149.6, 149.3, 140.8, 139.7, 139.5, 135.5, 134.8, 131.1, 130.3, 130.2, 129.0, 129.0, 127.9, 126.1, 125.7, 125.4, 124.1, 124.0, 117.0, 52.4, 49.5, 37.9, 28.9, 20.5, 19.9, 8.3. MS (ESI positive): 594 (M+H)⁺.

5.1.15. General procedure for hydrolysis of ester group of 16a–e, 17c–e

To a solution of ester (0.028 mmol) in THF (1.5 mL) and MeOH (1.5 mL) was added 1 N NaOH (0.084 mL, 0.084 mmol) and the mixture was stirred at rt overnight. The mixture was poured into satd NH₄Cl aq solution and the products were extracted with CH₂Cl₂. The extracts were dried over anhydrous MgSO₄ and concentrated. The obtained residue was purified by preparative TLC (CHCl₃/MeOH = 10:1) to afford carboxylic acid.

5.1.16. 4'-{1-Ethyl-1-[4-((E)-3-ethyl-3-hydroxy-1-pentenyl)-3-methylphenyl]propyl}-2'-methylbiphenyl-4-carboxylic acid (7a)

The yield was 60%. Colorless oil. ¹H NMR (CDCl₃) δ: 0.67 (6H, t, J = 7.2 Hz), 0.93 (6H, t, J = 7.5 Hz), 1.66 (4H, q, J = 7.5 Hz), 2.13 (4H, q, J = 7.2 Hz), 2.25 (3H, s), 2.34 (3H, s), 6.03 (1H, d, J = 15.9 Hz), 6.77 (1H, d, J = 16.1 Hz), 6.97–7.02 (2H, m), 7.06 (1H, dd, J = 7.9, 1.8 Hz), 7.09–7.13 (2H, m), 7.34 (1H, d, J = 7.8 Hz), 7.45 (2H, d, J = 8.6 Hz), 8.15 (2H, d, J = 8.6 Hz). ¹³C NMR (CDCl₃) δ: 171.6, 148.4, 147.7, 147.5, 137.6, 135.9, 134.5, 134.1, 133.4, 130.1, 129.9, 129.9, 129.5, 128.9, 127.4, 126.0, 125.9, 125.8, 124.9, 76.1, 49.4, 33.3, 29.1, 20.8, 20.3, 8.5, 7.9. HRMS (ESI negative): Calcd for C₃₃H₃₉O₃ 483.2905. Found: 483.2901 (M–H)[–].

5.1.17. 4'-{1-Ethyl-1-[4-((E)-3-ethyl-3-hydroxy-1-pentenyl)-3-methylphenyl]propyl}-2'-methylbiphenyl-3-carboxylic acid (7b)

The yield was 61%. Colorless oil. ¹H NMR (CDCl₃) δ: 0.67 (6H, t, J = 7.2 Hz), 0.93 (6H, t, J = 7.5 Hz), 1.66 (4H, q, J = 7.6 Hz), 2.13 (4H, q, J = 7.3 Hz), 2.24 (3H, s), 2.34 (3H, s), 6.03 (1H, d, J = 15.9 Hz), 6.77 (1H, d, J = 15.9 Hz), 6.99–7.02 (2H, m), 7.06 (1H, dd, J = 7.9, 1.8 Hz), 7.08–7.13 (2H, m), 7.34 (1H, d, J = 8.6 Hz), 7.50 (1H, t, J = 7.7 Hz), 7.59 (1H, d, J = 7.8 Hz), 8.07 (1H, d, J = 7.6 Hz), 8.10 (1H, s). ¹³C NMR (CDCl₃) δ: 171.6, 148.1, 147.6, 142.4, 137.6, 135.9, 134.6, 134.5, 134.2, 133.4, 131.1, 130.1, 129.9, 129.1, 129.0, 128.3, 128.2, 126.0, 125.9, 125.8, 124.9, 76.1, 49.4, 33.3, 29.1, 20.7, 20.3, 8.5, 7.9. HRMS (ESI negative): Calcd for C₃₃H₃₉O₃ 483.2905. Found: 483.2904 (M–H)[–].

5.1.18. 4'-{1-Ethyl-1-[4-((E)-3-ethyl-3-hydroxy-1-pentenyl)-3-methylphenyl]propyl}-2'-methylbiphenyl-4-yl)acetic acid (7c)

The yield was 76%. Colorless oil. ¹H NMR (CDCl₃) δ: 0.66 (6H, t, J = 7.2 Hz), 0.92 (6H, t, J = 7.5 Hz), 1.65 (4H, q, J = 7.5 Hz), 2.12 (4H, q, J = 7.3 Hz), 2.23 (3H, s), 2.33 (3H, s), 3.70 (2H, s), 6.02 (1H, d, J = 15.9 Hz), 6.76 (1H, d, J = 16.1 Hz), 6.98–7.03 (3H, m), 7.05–7.10 (2H, m), 7.31 (4H, d, J = 1.7 Hz), 7.33 (1H, d, J = 7.8 Hz). ¹³C NMR (CDCl₃) δ: 176.8, 147.6, 147.5, 141.0, 138.3, 135.8, 134.4, 134.1, 133.3, 131.4, 129.9, 129.6, 129.0, 128.9, 126.0, 125.9, 125.7, 124.9, 76.1, 49.3, 40.6, 33.3, 29.1, 20.8, 20.3, 8.5, 7.9. HRMS (ESI negative): Calcd for C₃₄H₄₁O₃ 497.3061. Found: 497.3051 (M–H)[–].

5.1.19. 4'-{1-Ethyl-1-[4-((E)-3-ethyl-3-hydroxy-1-pentenyl)-3-methylphenyl]propyl}-3-fluoro-2'-methylbiphenyl-4-yl)acetic acid (7d)

The yield was 79%. Colorless oil. ¹H NMR (CDCl₃) δ: 0.65 (6H, t, J = 7.1 Hz), 0.92 (6H, t, J = 7.4 Hz), 1.64 (4H, q, J = 7.3 Hz), 2.11 (4H, q, J = 7.2 Hz), 2.23 (3H, s), 2.33 (3H, s), 3.75 (2H, s), 6.02 (1H, d, J = 16.0 Hz), 6.76 (1H, d, J = 16.0 Hz), 6.96–7.09 (7H, m), 7.29 (1H, d, J = 7.8 Hz), 7.32 (1H, d, J = 8.0 Hz). ¹³C NMR (CDCl₃) δ: 175.9, 159.4, 148.0, 147.5, 143.6, 137.2, 135.8, 134.5, 134.1, 130.9, 130.0, 129.9, 128.9, 126.0, 125.9, 125.8, 125.2, 124.9, 118.6, 116.4, 76.1, 49.3, 33.9, 33.3, 29.1, 20.8, 20.3, 8.5, 7.9. HRMS (ESI negative): Calcd for C₃₄H₄₀FO₃ 515.2956. Found: 515.2956 (M–H)[–].

5.1.20. [6-(4-{1-Ethyl-1-[4-((E)-3-ethyl-3-hydroxy-1-pentenyl)-3-methylphenyl]propyl]-2-methylphenyl}pyridin-3-yl)acetic acid (7e)

The yield was 65%. Colorless oil. ¹H NMR (CDCl₃) δ: 0.65 (6H, t, J = 7.2 Hz), 0.92 (6H, t, J = 7.4 Hz), 1.64 (4H, q, J = 7.4 Hz), 2.11 (4H, q, J = 7.2 Hz), 2.30 (3H, s), 2.32 (3H, s), 3.70 (2H, s), 6.02 (1H, d, J = 15.8 Hz), 6.75 (1H, d, J = 16.0 Hz), 6.97–7.01 (2H, m), 7.05–7.09 (2H, m), 7.26 (1H, d, J = 7.2 Hz), 7.31 (1H, d, J = 7.8 Hz), 7.39 (1H, d, J = 8.0 Hz), 7.71 (1H, d, J = 7.4 Hz), 8.59 (1H, s). ¹³C NMR (CDCl₃) δ: 174.3, 158.8, 149.4, 148.9, 147.5, 137.3, 136.7, 134.8, 134.5, 133.4, 130.4, 130.0, 129.0, 128.8, 126.0, 125.8, 125.5, 124.8, 124.0, 76.0, 49.4, 37.7, 33.3, 29.1, 20.6, 20.3, 8.4, 7.9. HRMS (ESI negative): Calcd for C₃₃H₄₀NO₃ 498.3003. Found: 498.3016 (M–H)[–].

5.1.21. 4'-{1-Ethyl-1-[3-methyl-4-((E)-4,4,4-trifluoro-3-hydroxy-3-trifluoromethyl-1-butenyl]phenyl]propyl}-2'-methylbiphenyl-4-yl)acetic acid (8c)

The yield was 78%. Colorless oil. ¹H NMR (CDCl₃) δ: 0.65 (6H, t, J = 7.1 Hz), 2.11 (4H, q, J = 7.3 Hz), 2.21 (3H, s), 2.35 (3H, s), 3.68 (2H, s), 6.08 (1H, d, J = 16.1 Hz), 6.99 (1H, dd, J = 8.1, 1.7 Hz), 7.01–7.04 (2H, m), 7.04–7.09 (2H, m), 7.29 (4H, d, J = 2.0 Hz), 7.36 (1H, d, J = 7.8 Hz), 7.37 (1H, d, J = 16.1 Hz). ¹³C NMR (CDCl₃) δ: 177.6, 150.0, 147.2, 141.0, 138.4, 135.6, 135.2, 134.3, 132.2, 131.4, 130.8, 130.2, 129.9, 129.6, 129.1, 129.0, 126.3, 125.6, 125.4, 121.4, 116.4, 49.5, 40.7, 29.0, 20.8, 20.0, 8.4. HRMS (ESI negative): Calcd for C₃₂H₃₁F₆O₃ 577.2183. Found: 577.2195 (M–H)[–].

5.1.22. 4'-{1-Ethyl-1-[3-methyl-4-((E)-4,4,4-trifluoro-3-hydroxy-3-trifluoromethyl-1-butenyl]phenyl]propyl}-3-fluoro-2'-methylbiphenyl-4-yl)acetic acid (8d)

The yield was 95%. Colorless oil. ¹H NMR (CDCl₃) δ: 0.65 (6H, t, J = 7.0 Hz), 2.12 (4H, q, J = 6.9 Hz), 2.23 (3H, s), 2.36 (3H, s), 3.75 (2H, s), 6.09 (1H, d, J = 15.8 Hz), 6.99–7.10 (7H, m), 7.29 (1H, d, J = 7.8 Hz), 7.37 (1H, d, J = 7.8 Hz), 7.38 (1H, d, J = 16.4 Hz). ¹³C NMR (CDCl₃) δ: 176.2, 159.4, 149.9, 147.7, 143.5, 143.5, 137.4, 135.6, 135.2, 134.2, 130.9, 130.9, 130.8, 130.2, 130.0, 129.0, 126.3, 125.7, 125.5, 125.2, 125.2, 118.8, 116.4, 116.2, 49.5, 34.0, 29.0, 20.8, 20.0, 8.4. HRMS (ESI negative): Calcd for C₃₂H₃₀F₇O₃ 595.2078. Found: 595.2090 (M–H)[–].

5.1.23. [6-(4-{1-Ethyl-1-[3-methyl-4-((E)-4,4,4-trifluoro-3-hydroxy-3-trifluoromethyl-1-butenyl]phenyl]propyl]-2-methylphenyl}pyridin-3-yl)acetic acid (8e)

The yield was 40%. Colorless oil. ¹H NMR (CDCl₃) δ: 0.64 (6H, t, J = 7.1 Hz), 2.12 (4H, q, J = 14.5 Hz), 2.24 (3H, s), 2.29 (3H, s), 3.63 (2H, s), 6.06 (1H, d, J = 15.8 Hz), 6.98–7.06 (4H, m), 7.29–7.32 (2H, m), 7.34–7.37 (2H, m), 7.72 (1H, dd, J = 8.1, 1.7 Hz), 8.52 (1H, s). ¹³C NMR (CDCl₃) δ: 174.5, 158.0, 150.5, 149.7, 148.9, 148.6, 138.1, 136.0, 135.6, 135.1, 134.9, 131.0, 130.2, 129.1, 128.9, 128.1, 128.0, 126.2, 125.7, 125.5, 125.4, 124.4, 117.0, 49.5,

37.9, 28.8, 20.4, 19.9, 8.3. HRMS (ESI negative): Calcd for $C_{31}H_{30}F_6O_3$ 578.2124. Found: 578.2127 (M–H)[–].

5.2. VDRE reporter gene assay

MG-63 cells were plated at 2×10^3 cells/200 μ L/well in a 96-well white cell-culture plate and were incubated at 37 °C in 5% CO₂ for 24 h. Then, the MG-63 cells were cotransfected with 0.05 μ g of the pGV2-basic/VDRE-luciferase vector which contained three repeats of the VDRE sequence from mouse osteopontin promoter and 0.001 μ g of pRL-SV40 vector (Promega Corporation, WI, USA) using Lipofectamine (Invitrogen). The cells were added to minimum essential medium (MEM) containing 5% fetal bovine serum treated with dextran-coated charcoal (DCC-FBS) and were incubated for 8 h. The cells were treated with the serial diluted compounds (final concentrations were 10^{-7} to 10^{-11} mol/L with 0.1% DMSO) and were incubated for an additional 3 days. After removing the supernatants, the cells were lysed in cell-lysis buffer and luciferase activity was measured by DLR™ Assay System (Promega Corporation, WI, USA) and the luminescence was detected by Wallac ALVO SX 1420 multi-label counter (PerkinElmer, Inc., MA, USA). The half maximal effective concentrations (EC₅₀) were determined and the inductive activity was calculated as the ratio of the EC₅₀ value of the compounds to that of 1,25(OH)₂D₃ (Solvay Pharmaceuticals, Weesp, The Netherlands), which was used as a positive control.

5.3. Osteocalcin induction assay

MG-63 cells were plated at 2×10^3 cells/well in 200 μ L of serum-free MEM in a 96-well plate and were incubated at 37 °C in 5% CO₂ incubator for 24 h. After washing cells with 5% DCC-FBS/MEM (culture medium), the cells were added to culture medium and treated with the serial diluted compounds (final concentrations were 10^{-7} to 10^{-11} mol/L with 0.1% DMSO), and incubated for 8 h. After changing the culture medium to a fresh one, the cells were incubated for an additional 4 days, and then supernatant was collected and stored at –80 °C.

The frozen supernatant was thawed slowly at rt and Gla-type osteocalcin EIA kit (Takara Bio. Inc., Tokyo, Japan) was used to measure osteocalcin. Absorbance at 450 nm was measured on a plate reader (Model 3550, Bio-Rad Laboratories, CA, USA) and each concentration was calculated by comparison with standards using uplate Manager III software (Bio-Rad Laboratories). The EC₅₀ value was determined and the inductive activity was calculated as the ratio of the EC₅₀ value of the compounds to that of 1,25(OH)₂D₃.

5.4. Bone mineral density and serum calcium evaluation in the ovariectomized 8-week-old rats

Sham-operated ($n = 6$) and ovariectomized eight-week-old female Sprague–Dawley (Crj: CD (SD)) rats (Charles River Japan, Inc.) were used. One day after the surgery, the OVX rats were divided into each groups ($n = 6$), and were given compounds orally (25 and 50 ng/kg for **7c**, 10, 20, and 40 ng/kg for **7e**, 10 and 30 ng/kg for **8c**, or 20 and 60 ng/kg for **8d**, five times per week) or vehicle (medium-chain triglyceride (MCT), 1 mL/kg, five times per week) for 4 weeks. Vehicle-administered OVX rats and sham-operated rats served as controls. After 24 h from the last administration, blood was drawn from the abdominal aorta under ether anesthesia. Serum was collected after the blood sample had been centrifuged and was stored at –20 °C. The right femur was stored in 70% ethanol at 4 °C. Serum calcium concentrations were measured by an autoanalyzer (Hitachi 7170, Tokyo, Japan). The BMD in distal femur was measured by dual-energy X-ray absorptiometry (DCS-600-EX, Aloka, Japan).

5.5. Bone mineral density and serum calcium evaluation in the ovariectomized eight-month-old rats

Sham-operated ($n = 8$) or ovariectomized, eight-month-old, female, Sprague–Dawley (Crj: CD (SD)) rats (Charles River Japan, Inc.) were used. One day after the surgery, the OVX rats were divided into six groups ($n = 8$), and compound **7e** (0.75, 1.5, 3.0, 6.0, 12 ng/kg, five times per week) or vehicle (medium-chain triglyceride (MCT), 1 mL/kg, five times per week) was orally administered for 4 weeks.^{13,32} Vehicle-administered OVX rats and sham-operated rats served as controls. After 24 h from the last administration, blood was drawn from the abdominal aorta under ether anesthesia. Serum was collected after the blood sample had been centrifuged and was stored at –20 °C. The right femur and lumbar vertebrae (L2–L5) were stored in 70% ethanol at 4 °C. Serum calcium concentrations were measured by an autoanalyzer (Hitachi 7170, Tokyo, Japan). BMD in the distal femur and lumbar spine was measured by dual-energy X-ray absorptiometry (DCS-600-EX, Aloka, Japan).

5.6. Pharmacokinetic study

Compound **7e** in a dosing solution of ethanol/Tween20/saline (10:2:88) or ethanol/MCT (1:9) was administered to male Sprague–Dawley rats (8 weeks old, Orient Bio, Co.) under a fed condition at 100 μ g/kg intravenously or orally, respectively ($n = 3$). Blood samples were collected from the jugular vein and immediately centrifuged to obtain plasma samples. The compound in plasma was extracted with diethyl ether, and plasma concentration of the compound was measured by an API3000 tandem mass spectrometer (AB Sciex, Foster city, CA, USA) equipped with an Agilent 1100 liquid chromatography (Agilent Technologies, Santa Clara, CA, USA).

5.7. Crystallographic structure analysis

Protein sample preparation and crystallization were based on the methods by Moras and co-workers^{33,34} X-ray diffraction data collection and data processing were carried out by generally accepted methods. After brief soaking in the buffer containing 30% glycerol, 0.6 M ammonium sulfate and 0.1 M MES (pH6.3), crystals were trapped in the fiber loops and flash-cooled with liquid nitrogen. Crystals were stored and transported in a dry shipper. Data collections were carried out at the synchrotron beamline BL32B2 of the Spring-8 facility in Hyogo, Japan, operated by Pharmaceutical Consortium for Protein Structure Analysis. Crystals were kept frozen during data collection with a vapor stream from liquid nitrogen. X-ray diffraction data was collected with the R-AXIS V imaging plate area detector. The crystals were isomorphous with the space group P212121 reported by Moras and co-workers^{33,34} for the 1,25(OH)₂D₃–VDR complex. Data were processed with HKL2000. The initial structure model for the refinement was constructed by removing all the water and the ligand atoms in the 1,25(OH)₂D₃–VDR complex structure in the Protein Databank (PDB ID: 1db1). A rigid body refinement was followed by simulated annealing using the CNX. Electron density in the ligand-binding pocket clearly and unambiguously showed the ligand conformation. After fitting the ligand model into the electron density, structure refinement was continued with the software autoBUSTER and the water molecules were placed automatically. The data collection and the refinement statistics are summarized in Table 4.

5.8. Modeling

The compounds were manually docked in the crystal structure of VDR (PDB ID: 3W0C). The conformations of compounds were optimized using the MAB force field as implemented in the program MOLOC²⁸ with the VDR structure fixed.

Table 4
Crystal and diffraction data of VDR with compound **8d**

	8d
Wavelength (Å)	1.0
Cell (Å)	
(a)	45.2
(b)	51.1
(c)	132.7
Resolution (Å)	2.0
Completeness (last shell) (%)	90.4 (90.7)
Rsym (last shell) (%)	8.8 (32.8)
Rcryst (last shell) (%)	17.5 (18.6)
Rfree (last shell) (%)	20.9 (23.9)
Rmsd bond length (Å)	0.010
Rmsd bond angles (°)	0.99
No. of non-hydrogen protein atoms	1993
No. of water molecules	286

Acknowledgements

The authors thank Ms. Hitomi Suda of Chugai Pharmaceutical Co., Ltd, for HRMS measurements of the compounds and Editing Services of Chugai Pharmaceutical Co., Ltd, for proofreading the manuscript.

References and notes

- Sato, M.; Grese, T. A.; Dodge, J. A.; Bryant, H. U.; Turner, C. H. *J. Med. Chem.* **1999**, *42*, 1.
- Tilyard, M. W.; Spears, G. F.; Thomson, J.; Dovey, S. *N. Engl. J. Med.* **1992**, *326*, 357.
- Chapuy, M. C.; Arlot, M. E.; Duboeuf, F.; Brun, J.; Crouzet, B.; Arnaud, S.; Delmas, P. D.; Meunier, P. J. *N. Engl. J. Med.* **1992**, *327*, 1637.
- Dawson-Hughes, B.; Harris, S. S.; Krall, E. A.; Dallal, G. E. *N. Engl. J. Med.* **1997**, *337*, 670.
- Tanizawa, T.; Imura, K.; Ishii, Y.; Nishida, S.; Takano, Y.; Mashiba, T.; Endo, N.; Takahashi, H. *E. Osteoporos. Int.* **1999**, *9*, 163.
- Chapuy, M. C.; Pamphile, R.; Paris, E.; Kempf, C.; Schlichting, M.; Arnaud, P.; Garnero, P.; Meunier, P. J. *Osteoporos. Int.* **2002**, *13*, 257.
- Jackson, R. D.; LaCroix, A. Z.; Gass, M.; Wallace, R. B.; Robbins, J.; Lewis, C. E.; Bassford, T.; Beresford, S. A. A.; Black, H. R.; Blanchette, P.; Bonds, D. E.; Brunner, R. L.; Brzyski, R. G.; Caan, B.; Cauley, J. A.; Chlebowski, R. T.; Cummings, S. R.; Granek, L.; Hays, J.; Heiss, G.; Hendrix, S. L.; Howard, B. V.; Hsia, J.; Hubbell, F. A.; Johnson, K. C.; Judd, H.; Kotchen, J. M.; Kuller, L. H.; Langer, R. D.; Lasser, N. L.; Limacher, M. C.; Ludlam, S.; Manson, J. E.; Margolis, K. L.; McGowan, J.; Ockene, J. K.; O'Sullivan, M. J.; Phillips, L.; Prentice, R. L.; Sarto, G. E.; Stefanick, M. L.; Van, H. L.; Wactawski-W, J.; Whitlock, E.; Anderson, G. L.; Assaf, A. R.; Barad, D. *N. Engl. J. Med.* **2006**, *354*, 669.
- Holick, M. F. *Curr. Osteoporos. Rep.* **2006**, *4*, 96.
- Hayashi, Y.; Fujita, T.; Inoue, T. *J. Bone Miner. Metab.* **1992**, *10*, 50.
- Orimo, H.; Shiraki, M.; Hayashi, Y.; Hoshino, T.; Onaya, T.; Miyazaki, S.; Kurosawa, H.; Nakamura, T.; Ogawa, N. *Calcif. Tissue Int.* **1994**, *54*, 370.
- Okano, T.; Tsugawa, N.; Masuda, S.; Takeuchi, A.; Kobayashi, T.; Nishii, Y. *Contrib. Nephrol.* **1991**, *91*, 116.
- Tsurukami, H.; Nakamura, T.; Suzuki, K.; Sato, K.; Higuchi, Y.; Nishii, Y. *Calcif. Tissue Int.* **1994**, *54*, 142.
- Uchiyama, Y.; Higuchi, Y.; Takeda, S.; Masaki, T.; Shira-Ishi, A.; Sato, K.; Kubodera, N.; Ikeda, K.; Ogata, E. *Bone* **2002**, *30*, 582.
- Matsumoto, T.; Miki, T.; Hagino, H.; Sugimoto, T.; Okamoto, S.; Hirota, T.; Tanigawara, Y.; Hayashi, Y.; Fukunaga, M.; Shiraki, M.; Nakamura, T. *J. Clin. Endocrinol. Metab.* **2005**, *90*, 5031.
- Matsumoto, T.; Ito, M.; Hayashi, Y.; Hirota, T.; Tanigawara, Y.; Sone, T.; Fukunaga, M.; Shiraki, M.; Nakamura, T. *Bone* **2011**, *49*, 605.
- Sanford, M.; McCormack, P. L. *Drugs* **2011**, *71*, 1755.
- Sanford, M.; McCormack, P. L. *Drugs Aging* **2012**, *29*, 69.
- Boehm, M. F.; Fitzgerald, P.; Zou, A.; Elgort, M. G.; Bischoff, E. D.; Mere, L.; Mais, D. E.; Bissonnette, R. P.; Heyman, R. A.; Nadzan, A. M.; Reichman, M.; Allegretto, E. A. *Chem. Biol.* **1999**, *6*, 265.
- Swann, S. L.; Bergh, J.; Farach-Carson, M. C.; Ocasio, C. A.; Koh, J. T. *J. Am. Chem. Soc.* **2002**, *124*, 13795.
- Peräkylä, M.; Malinen, M.; Herzig, K. H.; Carlberg, C. *Mol. Endocrinol.* **2005**, *19*, 2060.
- Hosoda, S.; Tanatani, A.; Wakabayashi, K.; Nakano, Y.; Miyachi, H.; Nagasawa, K.; Hashimoto, Y. *Bioorg. Med. Chem. Lett.* **2005**, *15*, 4327.
- Ma, Y.; Khalifa, B.; Yee, Y. K.; Lu, J.; Memezawa, A.; Savkur, R. S.; Yamamoto, Y.; Chintalacheruvu, S. R.; Yamaoka, K.; Stayrook, K. R.; Bramlett, K. S.; Zeng, Q. Q.; Chandrasekhar, S.; Yu, X. P.; Linebarger, J. H.; Iturria, S. J.; Burris, T. P.; Kato, S.; Chin, W. W.; Nagpal, S. *J. Clin. Invest.* **2006**, *116*, 892.
- Hosoda, S.; Tanatani, A.; Wakabayashi, K.; Makishima, M.; Imai, K.; Miyachi, H.; Nagasawa, K.; Hashimoto, Y. *Bioorg. Med. Chem.* **2006**, *14*, 5489.
- Demizu, Y.; Takahashi, T.; Kaneko, F.; Sato, Y.; Okuda, Y.; Ochiai, E.; Horie, K.; Takagi, K.; Kakuda, S.; Takimoto-Kamimura, M.; Kurihara, M. *Bioorg. Med. Chem. Lett.* **2011**, *21*, 6104.
- Kashiwagi, H.; Ono, Y.; Shimizu, K.; Haneishi, T.; Ito, S.; Iijima, S.; Kobayashi, T.; Ichikawa, F.; Harada, S.; Sato, H.; Sekiguchi, N.; Ishigai, M.; Takahashi, T. *Bioorg. Med. Chem.* **2011**, *19*, 4721.
- Kashiwagi, H.; Ono, Y.; Ohta, M.; Morikami, K.; Takahashi, T. *Bioorg. Med. Chem.* **2012**, *20*, 4495.
- Kashiwagi, H.; Ohta, M.; Ono, Y.; Morikami, K.; Itoh, S.; Sato, H.; Takahashi, T. *Bioorg. Med. Chem.* **2013**, *21*, 712.
- Gerber, P. R.; Müller, K. J. *Comput. Aided Mol. Des.* **1995**, *9*, 251.
- Hourai, S.; Fujishima, T.; Kittaka, A.; Suhara, Y.; Takayama, H.; Rochel, N.; Moras, D. *J. Med. Chem.* **2006**, *49*, 5199.
- Suda, T.; Takahashi, F.; Takahashi, N. *Arch. Biochem. Biophys.* **2012**, *523*, 22.
- Taniguchi, K.; Katagiri, K.; Kashiwagi, H.; Harada, S.; Sugimoto, Y.; Shimizu, Y.; Arakawa, H.; Ito, T.; Yamazaki, M.; Watanabe, T.; Kato, A.; Hoshino, E.; Takahashi, T.; Esaki, T.; Suzuki, M.; Takeda, S.; Ichikawa, F.; Harada, A.; Sekiguchi, N.; Ishigai, M.; Kawata, H.; Yoneya, T.; Onuma, E.; Sudoh, M.; Aoki, Y. *Steroid Biochem. J. Mol. Biol.* **2010**, *121*, 204.
- de Fretas, P. H. L.; Hasegawa, T.; Takeda, S.; Sasaki, M.; Tabata, C.; Oda, K.; Li, M.; Saito, H.; Amizuka, N. *Bone* **2011**, *49*, 335.
- Juntunen, K.; Rochel, N.; Moras, D.; Vihko, P. *Biochem. J.* **1999**, *344*, 297.
- Rochel, N.; Wurtz, J. M.; Mitschler, A.; Klaholz, B.; Moras, D. *Mol. Cell* **2000**, *5*, 173.